Benzyl coupling on bismuth-modified Pt(111)

Mark A. Newton [1] and Charles T. Campbell

Department of Chemistry, The University of Washington, Seattle, WA 98195-1700, USA

Received 21 August 1995; accepted 23 October 1995

It has been found that adsorbed benzyl (ϕ-CH_2(a)), produced from methylcyclohexane, can undergo dimerisation to adsorbed bibenzyl (ϕ-CH_2-CH_2-ϕ) on a bismuth-modified Pt(111) surface. In this case, the bismuth was postdosed to the benzyl adlayer, as in bismuth postdosing thermal desorption mass spectroscopy (BPTDS). The bibenzyl product desorbs to give bibenzyl gas in good yield with respect to the starting benzyl or the reacted methylcyclohexane. This reaction competes poorly with simple hydrogenation of the benzyl species to toluene when adsorbed hydrogen is also present on the bismuth-dosed surface. In the absence of hydrogen, dimerization dominates the chemistry of this intermediate, although some direct desorption of benzyl radical also occurs. The dependence of the activation energy for benzyl coupling on the thickness of the bismuth film suggests that the bismuth resides between the Pt surface and the benzyl adlayer. Benzyl coupling and desorption occurs on Bi/Pt, whereas only its decomposition occurs on clean Pt. This is attributed to two effects: the weakness of C–Bi bond leads to a low barrier for benzyl coupling or desorption; and, (2) bismuth blocks Pt sites needed to stabilize the fragments of decomposition. Both D_2-BPTDS and this bismuth-induced coupling reaction in simple BPTDS were used to monitor the coverage of benzyl during its thermal decomposition on bismuth-free Pt(111), and the temperature dependence of the rate of its decomposition. Estimates of the bismuth–carbon bond strengths are also presented.

Keywords: platinum, bismuth modified; hydrocarbon synthesis; C–C bond-forming catalysts; bond strengths, carbon–metal; reforming reactions

Hydrocarbon chemistry, particularly on Pt, is a subject to which much attention has been devoted. Aside from the practical relevance of such studies in the catalytic reforming of crude oil fractions, such elementary reactions as C–C and C–H bond activation are legion. As such there is considerable fundamental interest in these processes [1], though the details of the reactions that break or form C–C bonds have proved somewhat difficult to investigate quantitatively on Pt in UHV. Bismuth deposited on Pt has also aroused interest in the field of electrochemistry [2] and, at least in one case, as a promoter in the selective catalytic oxidation of alcohols [3].

The deposition of Bi, particularly on Pt, has also emerged as a means to investigate some aspects of surface chemistry that are otherwise very difficult to determine, chiefly through its ability to stifle the C–H and C–C bond cleavage activity of the substrate Pt. As a result, questions regarding Pt ensemble sizes required for specific reactions of various hydrocarbons have been successfully addressed [4].

Further, by depositing $\geqslant 1$ ML of Bi to a previously treated adsorbate/Pt surface, any subsequent dissociative chemistry due to Pt is also curtailed. Any adsorbed *molecular* products of the previous treatment can therefore be desorbed intact and identified. It is this approach to species identification during the chemistry of complex molecules on Pt that is called bismuth postdosing thermal desorption mass spectroscopy (BPTDS) [5]. The utility of postdosed Bi in surface analysis even extends to reaction intermediates (*molecular fragments*) which are deficient in one hydrogen atom relative to a stable gas phase molecule: in the presence of surface deuterium or $D_{(a)}$, dosed after the initial hydrocarbon adlayer but before the Bi, such species will add one deuterium and desorb as monodeuterated (d_1) molecules. The identity of the original adsorbed radical can be inferred from the resulting cracking pattern of this deuterated adduct using a mass spectrometer. When D_2 is dosed before the Bi like this, we call the method D_2-BPTDS [5]

The species whose chemistry we shall probe here is an adsorbed benzyl species (ϕ-$CH_{2(a)}$, ϕ- being a phenyl ring (c-C_6H_5-). In the current case, it has been generated during, and identified as an important intermediate in, the thermal chemistry of methylcyclohexane (c-C_6H_{11}-CH_3) dosed to Pt(111) [6,7]. It can also be produced from the dehydrogenation of toluene on Pt(111) [5d,11]. In the absence of Bi on the Pt surface this benzyl intermediate, in common with most other adsorbed hydrocarbons, undergoes degradation to adsorbed carbon and $H_{2(g)}$ upon heating in ultrahigh vacuum (UHV). This degradation primarily proceeds through several steps of dehydrogenation and possibly also C–C bond cleavage; although we have recently demonstrated, using BPTDS, that a minor process on the Pt surface is a benzyl degradation route that has adsorbed benzene as its product [8].

In the current communication we show that an

[1] Currently at the Department of Chemistry, The University of Southampton, Highfield, Southampton, SO9 5NH, United Kingdom.

entirely new chemical option for the adsorbed benzyl species, dimerisation to bibenzyl, can be induced through the addition of Bi to the surface. Moreover, this species can be desorbed intact from the Bi/Pt(111) surface at relatively low temperatures. Using both this dimerization process and D_2-BPTDS, the kinetics of benzyl decomposition have also been monitored, and are reported here.

The experiments were carried out in a stainless steel vacuum chamber with a base pressure of $< 2 \times 10^{-10}$ mbar. The sample was cleaned using Ar ion sputtering and annealing at $\sim$ 1180 K. Low energy electron diffraction and Auger spectroscopy provided the means to assess surface cleanliness and long range order. Methylcyclohexane (MCH) was purified using freeze–pump–thaw cycles until no contaminants were detected and was dosed to the sample at 100 K. The adlayer was then subjected to thermal treatment, firstly to $\sim$ 380–420 K to generate the benzyl species and, at higher temperatures, to induce further chemistry. It should be noted that of the complete monolayer (ML) of MCH initially dosed, corresponding to $\sim$ 0.14 molecules per Pt(111) surface atom, only $\sim$ 35–40% remains irreversibly adsorbed and goes on to form adsorbed benzyl; the remainder desorbs intact during normal TPD [6,7]. The coverage of adsorbed benzyl used in these experiments is thus $\sim$ 0.049–0.056 species per Pt surface atom. This thermal treatment produces this adsorbed benzyl in fairly pure form since the hydrogen adatoms, generated from MCH when it dehydrogenates to benzyl, also desorb as H_2 gas during the initial heating to $\sim$ 380–420 K [6,7]. Subsequent to this thermal treatment, the sample was cooled to 100 K and then dosed with Bi at predetermined levels. A range of Bi coverages was eventually used, from 0–2 ML. In D_2-BPTDS, D_2 was dosed to the surface just before the Bi. The requirement for the D_2 dose was that, where used, it should merely create $D_{(a)}$ in excess. The resulting complex surface was then subjected to rapid heating (5.5 K s^{-1}) whilst the species desorbing from the surface were monitored using a quadrupole mass spectrometer (QMS) multiplexed to follow up to six masses simultaneously and interfaced to a computer.

The mass spectral cracking patterns measured in our instrument are very similar to those reported in the literature [10], except for a more rapid decrease in intensity with m/e. The mass spectral cracking patterns for several C_6, C_7, C_8 and C_{14} hydrocarbons were determined by flowing a pure sample of each hydrocarbon through the chamber. The measured spectrum was compared to the literature spectra in each case by normalizing the spectral intensities near $m/e = 39$ to 1.00. The ratio of intensities of all other observed peaks to that in the literature cracking pattern was plotted versus m/e ratio, and found to decrease smoothly but rapidly with mass. The plot included numerous hydrocarbons, and all masses up to 200. It was well fitted by the function $4\exp(-0.04m/e)$. The error was within the scatter of the data, or the reproducibility of literature cracking patterns. (Different literature cracking patterns for the same molecule often give relative intensities for small peaks that differ by a factor of up to two [10].) This steep function reflects the poor transmission function of our mass spectrometer at high masses. We have used it routinely in other studies to correct literature cracking patterns for the transmission function of our mass spectrometer, and the resulting spectra agree well with what we measure. This function sets the practical upper mass limit of our mass spectrometer in TPD applications for submonolayer amounts of hydrocarbons at about m/e = 100–150, depending on the relative intensity of the ion. Intensities for higher masses are often at the noise level with such small amounts of desorbing molecules. The stated upper mass limit of the mass spectrometer, however, is 200 amu.

Figs. 1a and 1b show typical BPTDS and D_2-BPTDS spectra, respectively, obtained for a number of masses. In these experiments, the crystal was initially "flashed" to $\sim$ 420 K, subsequent to dosing 1 ML at 100 K of MCH. After recooling to 100 K, it was subjected to the relevant BPTDS or D_2-BPTDS methodology. Other masses will be discussed below, though for current purposes those in fig. 1 show the main trends. Species identification was based on the relative intensities of between eight and fifteen masses. These intensities would then be compared (after correction for the mass transmission function [9] of our mass spectrometer) to cracking pattrens available in the literature [10], or to those collected previously on our system.

The most striking observation to be made immediately is the effect that postdosed D_2 has on the absolute intensities of the various desorption features present in the spectra. The peak for mass 78 desorbing at $\sim$ 190 K is unaffected. In stark contrast to this, the relative intensities of the features at $\sim$ 210 K and the feature(s) at $\sim$ 300–400 K are strongly affected by the lack, or presence, of adsorbed deuterium. The reasons for mass 78 actually being desorbed, and for its insensitivity to the presence of postdosed D_2 have been dealt with elsewhere [8]. It is due to a minor amount of adsorbed benzene produced from the decomposition of adsorbed benzyl [8]. The feature at $\sim$ 220 K in fig. 1b, characterised by the coincident desorption of masses 93, 92, 91 (and others), is confirmed as being due to the desorption of d_1-toluene through reference to the known mass spectrum of this compound. It is derived from the deuteration of benzyl species left after thermal treatment of the MCH-dosed Pt surface. This has been previously observed for this system [7] and in D_2-BPTDS from toluene dosed Pt(111) for pre-treatment temperatures of $\sim$ 350 to 470 K [5d]. The η^7-adsorbed benzyl species was first identified in this system using HREELS [11]. Having identified this feature as such, it is therefore no great surprise to see it disappear in the absence of postdosed D_2. In addition to

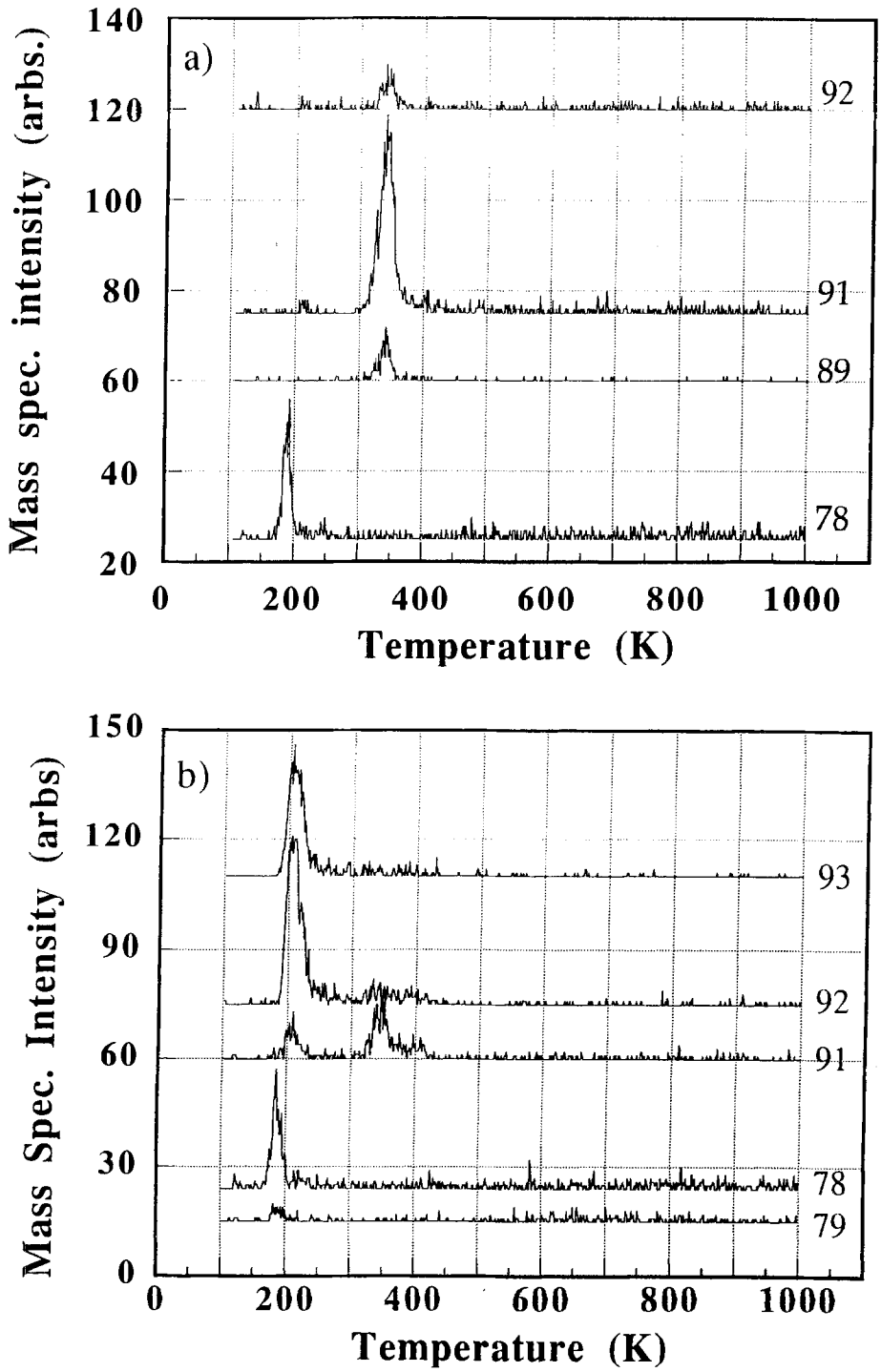

Fig. 1. (a) BPTDS results obtained after flashing a layer of ~ 2/3 monolayer of MCH, initially adsorbed at 100 K, to ~ 425 K. Subsequent to this flash the sample was cooled again to 100 K, Bi was dosed, and a thermal ramp was applied. The signals shown here were obtained at this second thermal treatment. The masses of each trace are indicated. (b) As (a) but with addition of a 10 L D_2 dose to the surface after the flash to 425 K, but prior to Bi adsorption and the subsequent thermal ramp. This addition D_2 to the sequence is referred to as D_2-BPTS.

these species, there is a high temperature (300–420 K) mass 91 feature in both BPTDS and D_2-BPTDS (figs. 1a and 1b).

Fig. 2 shows the dependence of the integrated intensity of this high temperature (300–420 K) mass 91 feature on the preliminary flash temperature, for both BPTDS and D_2-BPTDS, along with the intensity of the 210 K mass 93 desorption peak in D_2-BPTDS experiments. This mass 93 peak reflects d_1-toluene amounts, and serves to show the relative levels of benzyl at the surface for a given flash temperature. The similarity between this trace and that of the high temperature mass 91 peak tells us that whatever is desorbing between 300 and 420 K as mass 91 is closely related to the amount of

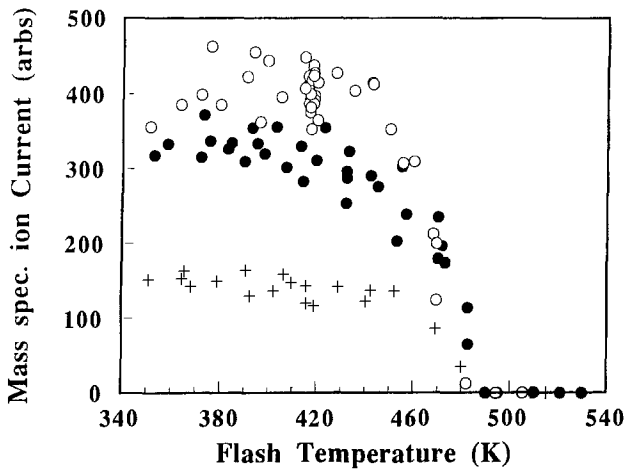

Fig. 2. Dependence of the intensities of the low temperature (~ 210 K) peak due to d_1-toluene desorption in D_2-BPTDS (mass 92, solid circles) and the high temperature (300–400 K) mass 91 desorption (BPTDS: open circles; D_2-BPTDS: crosses) on the pre-flash temperature of the MCH adlayer.

benzyl at the surface. This is confirmed by noting, as suggested in fig. 1 but shown clearly here, that this high temperature desorption peak is severely attenuated when the low temperature route for removal of the benzyl as d_1-toluene is possible. That it is not removed completely would seem to indicate, given that $D_{(a)}$ is present in excess at the surface, that the chemistry leading to the mass 91 desorption can, to some extent, compete with the simple deuteration reaction. The dependence on the level of mass 91 on the presence of deuterium in the experiment also tells us that, whatever is desorbing it is not made during the initial flash. If it were made during the initial thermal treatment of the surface, then the amount of it desorbing would be independent of the presence of $D_{(a)}$ at the surface.

The desorption in the higher temperature range of 300–420 K is somewhat surprising, but what is desorbing? The relative intensities in this feature of some of the key masses needed in identifying potential products are presented in table 1, along with the known cracking patterns of potential products that might evolve from adsorbed benzyl. Literature cracking patterns presented in table 1 have been scaled by the factor $\exp(-0.04m/e)$ to correct for the relative transmission function of our mass spectrometer (see above). The average BPTDS peak areas, integrated between 300 and 450 K from experiments like those in figs. 1a and 2, are presented here. Note that, by comparing these relative intensities, it is trivial to rule out toluene: the 92 : 91 ratio is way too low. Indeed, the mass spectrum of no C_7 hydrocarbon species available in the literature [10] gives any reasonable comparison to this observed ratio of masses. Also, the 89 : 91 ratio is way too low for stilbene. The only stable hydrocarbon that matches at all well the ion distribution seen in this desorption feature is bibenzyl (ϕ-CH_2-CH_2-ϕ), the product of simple dimerisation between two benzyl species. Since our mass spectrometer has a very rapidly decreasing transmission function with increasing mass, the intensity in the cracking pattern for this amount of bibenzyl at masses > 100 would be below our noise level (see above). Thus, the parent ion could not be used for its further identification. Because of the reasonable agreement with bibenzyl, we will conclude it is the main species here.

However, there are other species desorbing here as well, since the relative intensities at masses 65, 89 and 92 are too large for pure bibenzyl. The additional intensity at mass 65 and 89 can be attributed to simultaneous desorption of gaseous benzyl radical, as can be seen by comparison to the cracking pattern of benzyl radical in table 1. (Note that the cracking patterns of the benzyl radical entered in table 1 were generated by Turecek et al. [20,21] using neutralization/reionization mass spectroscopy, in parentheses, and by collisional-induced dissociation of the bibenzyl cation radical followed by reionization of the benzyl radical by collision with oxygen. These schemes give different relative intensities for the ions than obtained by normal ionization with electron impact, due to the difference in energy content of the parent benzyl. However, they show the trend that the fragment ions have far more intensity relative to the par-

Table 1
Identification of 300–420 K BPTDS peaks

m/e	Observed intensity	Known cracking patterns (transmission-corrected)			
		bibenzyl	benzyl [a]	toluene [b]	stilbene [b]
92	0.21 ± 0.02	0.065	0.07 (0.07)	0.69	0
91	1.00	1.00	1.00	1.00	0.2
89	0.16 ± 0.01	0.024	0.51 (2.0)	0.044	3.0
78	0.045 ± 0.025	0.022	0.16 (0)	0	0.48
77	0.020 ± 0.015	0.039	0.17 (0)	0.02	1.3
65	1.18 ± 0.22	0.33	1.2 (2.8)	0.39	0.5
52	0.15 ± 0.03	0.04	0.45 (2)	0.1	0.5
51	0.30 ± 0.24	0.17	2.00 (10)	0.5	2.5

[a] These values for benzyl radical were obtained by a different method, and are taken from ref. [21], after correcting for transmission. (Numbers in parentheses are from ref. [20], corrected for transmission.)

[b] From ref. [10], after correcting for transmission. (The transmission function correction is $4\exp(-0.04m/e)$: see text.)

ent in the spectra of benzyl radical than in bibenzyl. This trend is also expected when comparing normal electron ionization spectra, since each benzyl carries only about half the ionization energy when bibenzyl is ionized, whereas all this energy must be carried by a single benzyl when starting with the benzyl radical, thus leading to more fragmentation.) Thus, the additional intensities at lower masses can be explained by the additional presence of some amount (10–40%) of benzyl radical. (The observed intensities of most of the lower masses relative to mass 91 is too small for this peak to contain more than about 40% benzyl radical, judging by the literature cracking patterns presented in table 1.) The additional mass 92 observed could be due to a low level ($\sim$ 15%) of toluene, perhaps created by hydrogenation of this same benzyl radical upon collision with the walls of the chamber. Methane is produced by such wall reactions when methyl desorbs from gold surfaces, giving a mass 16 peak that is $\sim$ 1/3 the mass 15 intensity [27]. Below we will show why benzyl radical desorption might be kinetically competitive with benzyl dimerisation, even at this low temperature.

Along with the striking dependence of the intensity of the feature attributed mainly to bibenzyl on the presence of $D_{(a)}$, there is a second feature within fig. 1 that is noteworthy. In fig. 1b two (albeit ill defined) desorption features appear present, most notably in mass 91; in fig. 1a however only one is obvious. The change in the number of bibenzyl desorption peaks points to variations in the surface treatment, subsequent to the thermal treatment of the adsorbate covered surface, having a marked effect on how the bibenzyl desorbs from the surface. As we will show, this is due to small changes in the bismuth coverage used here (near one ML). The number of bibenzyl desorption peaks is reproducible, but heavily dependent upon the level of Bi at the surface, as we will show next.

Fig. 3 shows the effect of varying the amount of Bi, dosed to one ML of MCH that had been pretreated to 425 K, on the production and desorption of the bibenzyl. The pretreatment of MCH to $\sim$ 425 K produces adsorbed benzyl, and removes all the resulting $H_{(a)}$ as $H_{2(g)}$. No deuterium has been added in these cases. Using Auger spectroscopy and Bi TPD, it was found that, under the conditions employed, 1 ML of Bi was deposited in $\sim$ 4.0 min. The bottom spectrum, corresponding to $\sim$ 1/2 ML of Bi (2 min deposition), results in a spectrum with three peaks at $m/e = 91$: a small peak at $\sim$ 200 K and strong peaks at $\sim$ 300 and 420 K. The relative ratios of masses 92 (not shown) and mass 91, as well as comparison of this spectrum to toluene molecular desorption from Pt(111) [5d,11] show that, where a submonolayer amount of Bi has been deposited, the desorption observed is predominantly of toluene. From spectra at intermediate coverages, it is clear that some bibenzyl is also present when the Bi coverage exceeds about 1/2 ML but is less than 1 ML.

There are two possible reasons for the desorption of toluene in this bottom spectrum; these are related to there being a relatively large number of free Pt sites at the surface at this submonolayer Bi dose. First, this may allow some degree of dissociative adsorption of hydrogen impurity from the background; this hydrogen can then hydrogenate adsorbed benzyl species and form

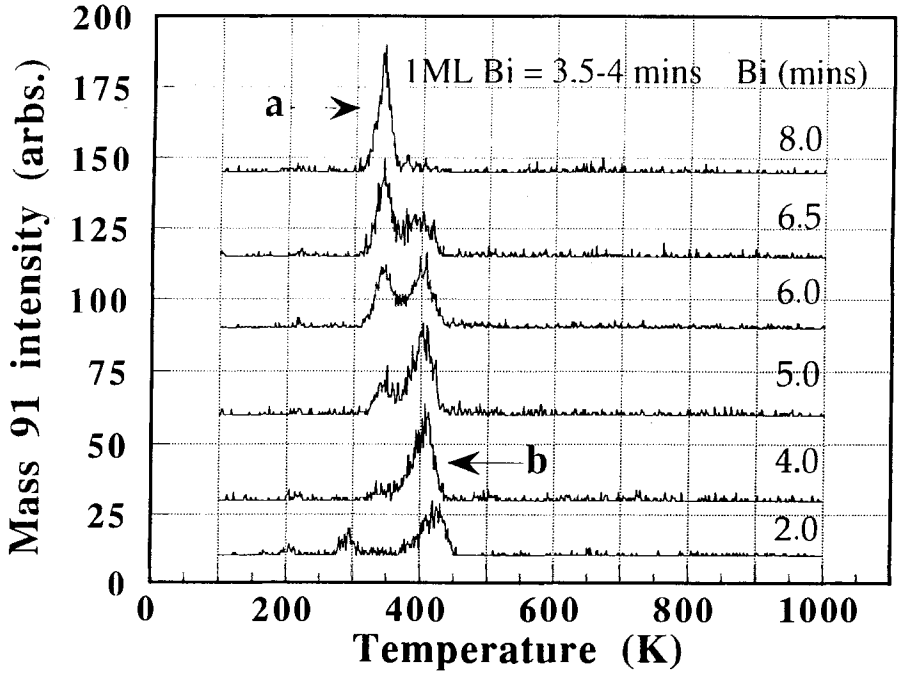

Fig. 3. Dependence of the high temperature mass 91 desorption features (BPTDS only) on the Bi deposition time used. In each case the monolayer of MCH (adsorbed at 100 K) was flashed to a temperature of $\sim$ 420 K before subsequent Bi adsorption and thermal ramp.

toluene, as we have already seen. The second effect could be some partial dehydrogenation of the benzyl species occurring during heating at low Bi levels. This too would release surface hydrogen which could trap any available benzyl species and form toluene. Estimates of the level of H_2 adsorption from its low background partial pressure suggest that the second effect is by far larger.

At $\sim$ 1 ML coverage of Bi the situation has changed. The three-peak spectrum has been replaced by a single peak. The ratios of masses 89, 91, and 92 are now like those in table 1, showing that this is now desorption of mainly bibenzyl (plus some benzyl radical), with a peak temperature (T_{max}) of $\sim$ 410 K. Increasing the dose of Bi beyond 1 ML causes the appearance of a second desorption feature at lower peak temperature: $T_{max} \sim 340$ K. As the Bi dose increases towards 8 min the lower temperature peak (b) increases at the expense of the higher temperature peak (a) until, at 8 min, only the lower temperature (b) state remains. Integration of the peaks due to bibenzyl in the region 300–450 K shows that after the deposition of $\geqslant$ 1ML of Bi, the total amount of bibenzyl desorbed is nearly constant despite the intensity within the individual peaks shifting from the (a) state to the (b) state as the Bi coverage increases.

Thus on clean Pt(111), and at $< 1/2$ ML coverage of Bi, dimerisation is not part of the chemistry available to adsorbed benzyl species. Upon the formation of $\geqslant$1ML of Bi on the Pt surface (from fig. 3) the dimerisation becomes probable and so does the desorption of this large molecule. Hence alongside the known ability of adsorbed Bi to induce desorption of adsorbates bound to Pt instead of decomposition, it appears that Bi can induce new reactions that are unavailable on the clean surface, such as dimerization.

BPTDS shows no desorption products other than those due to bibenzyl or the small amounts of benzyl, toluene and benzene mentioned above and in ref. [8]. At preflash temperatures below which the adsorbed benzyl starts to degrade (340–420 K), there is also no high temperature (> 800 K) H_2 desorption peak in the BPTDS [5e]. This high temperature H_2 BPTDS peak would be seen if a portion of the benzyl or other hydrocarbon fragments were left on the surface until high temperature [5f], for it would dehydrogenate when the Bi finally started to desorb (> 850 K) [5f]. The circumstantial conclusion is that, in the absence of adsorbed hydrogen, a high proportion of the adsorbed benzyl undergoes the observed dimerisation reaction (with some direct radical desorption). We shall present other indirect evidence below that also strongly supports this suggestion.

A number of further questions also remain. How has this new chemistry arisen? How do we explain the changes in the bibenzyl desorption as the Bi coverage is altered? Lastly, when does the C–C bond formation which leads to bibenzyl occur?

Taking the latter first, the chemistry of bibenzyl on Pt(111) has been extensively investigated [5e]. In BPTDS, subsequent to the adsorption of bibenzyl at 100 K with no thermal pretreatment, two bibenzyl desorption features were observed. They were attributed to desorption of "fully" and "partially" bonded bibenzyl molecules. In this case, "fully" bonded refers to a near planar bonding wherein both phenyl rings are maximally bonded to the surface. "Partial" bonding refers to a less favorable arrangement wherein steric constraints at high bibenzyl coverage force the bibenzyl to adopt a less than optimal bonding arrangement. These two BPTDS features occur with peaks at $\sim$ 300 and 240 K respectively [5e]. If we assume a preexponential factor for desorption of 10^{13} s^{-1} [12], these peak temperatures give values of $\sim$ 77 and $\sim$ 60 kJ mol^{-1}, respectively, for the desorption activation energies, in BPTDS, of molecularly adsorbed bibenzyl. This is in contrast to the desorption temperatures of the bibenzyl features of $\sim$ 390 and 340 K reported in the current work, which give activation energies of $\sim$ 101 and 88 kJ mol^{-1}, respectively. An obvious difference in the two experiments is that in the previous work the bibenzyl has been adsorbed from the gas phase, whereas in the current experiment it is made from adsorbed benzyl even as the surface is being heated. The simplest explanation for the difference in desorption temperatures therefore is that in the former case the desorption peak maximum temperature reflects the kinetics of the desorption of the bibenzyl from the complex Bi covered surface, whilst the desorption temperatures in the current work reflect more the activation energies for the C–C bond formation processes leading to bibenzyl formation. This explains the fact that these peaks appear above the bibenzyl desorption temperature on these surfaces.

The dependence of the relative intensities of the two bibenzyl desorption states on the level of Bi in fig. 3 is therefore explainable as follows. At 1ML (4 min) Bi coverage we have generated a single layer of Bi that has uniformly interfered with the bonding of the benzyl to the Pt surface, resulting in all the benzyl species being equally destabilised. Thus either all the bibenzyl species are desorbed with the same barrier to formation/desorption; this results in a single desorption feature. As we deposit more Bi we create unequal areas on the surface. Some of the benzyl remains unaffected by the second layer of Bi, whereas a portion of the benzyl species are further destabilised through a further screening of the Pt by an additional layer of Bi (locally). Thus, they are even more readily created/desorbed, resulting in a second, lower temperature desorption peak for bibenzyl, alongside that peak due to patches covered by a single monolayer of Bi. As the second layer of Bi grows the chemistry due to the 1 ML Bi/Pt(111) areas gradually becomes a minority contributor, and more and more of the lower temperature feature, due to benzyl or bibenzyl species destabilised by 2 ML of Bi, becomes apparent. Finally at 8 min of Bi deposition, corresponding to roughly 2 ML of Bi, all the adsorbed benzyl has been

destabilised by the 2 ML of Bi and thus only the single, lower temperature desorption feature is observed.

Thus the dependence of the activation temperature for benzyl coupling on Bi coverage suggests that the bismuth resides *between* the Pt surface and the benzyl adlayer, at least by 300 K when coupling occurs. This helps us to understand how BPTDS operates. The postdosed Bi squeezes *between* adlayers and the transition metal. This greatly destabilizes the adspecies, permitting its low temperature desorption, deuteration, or coupling. In some previous cases [5a,5g], postdosed Bi has also been observed to squeeze between adsorbed hydrocarbons and the Pt substrate. This is energetically feasible: while it involves replacing hydrocarbon–Pt bonds with weaker hydrocarbon–Bi bonds, at the same time weak Bi–Bi bonds are replaced with much stronger Bi–Pt bonds [5a,5f,5g].

Another important point about the result of fig. 3 is the implication it has concerning the amount of bibenzyl gas that is produced. Note that in going from 1 ML of Bi to 2 ML of Bi, the amount of bibenzyl that is produced stays the same. It is produced, however, at a much lower temperature in the presence of 2 ML of Bi. If the reaction yield were not close to 100%, one would expect that this lowering in the activation barrier for benzyl coupling should lead to a marked increase in its yield. (That is, this path should become much more competitive with possible parallel reactions.) Since the yield does not change substantially, we can conclude that production of bibenzyl gas is the dominant reaction product for adsorbed benzyl in this Bi coverage range. This conclusion is not inconsistent with the magnitudes of the bibenzyl signals seen here compared to those measured during a previous investigation of bibenzyl chemistry on Pt(111) in this same chamber [5e], given possible changes that may have occurred in spectrometer tuning and sensitivity over the many months between these measurements. (Unfortunately, the sizes of these changes were not monitored, so this comparison of signal intensities is quite unreliable in the present case. Thus, we can only claim that the signal was of the proper order of magnitude for 100% yield.)

But why does this C–C bond forming reaction occur? The answer lies in the way that BPTDS is already known to work [5f]. First, Bi adatoms effectively block Pt sites needed for accommodating the fragments of adsorbed hydrocarbon decomposition (mainly dehydrogenation). In the manner that BPTDS has been used to date this is mainly reflected in the loss of any typical decomposition chemistry, which in this case involves further dehydrogenation of the benzyl species via dehydrogenation and possibly C–C bond scission. The postdosing of a full monolayer of Bi is also known to greatly destabilise adsorbed hydrocarbons [5]. In BPTDS, this results in a much lower desorption activation energy for molecularly adsorbed species, so that their molecular desorption now dominates over dehydrogenation. In the present case, the species (benzyl) is a molecular fragment rather than a molecule, so that its desorption (as a radical) might still take a relatively high temperature. In this case, other chemistry may occur before desorption, and indeed it does: dimerization also occurs, and it appears to be more important than direct desorption of the radical from the comparison of table 1.

When bismuth is postdosed, it appears that benzyl–Pt bonds are replaced with benzyl–Bi bonds. Carbon–bismuth bonds are well known to be very weak [13–15]. For example, the mean C–Bi bond energy in trimethyl bismuth is only 143 kJ/mol [13], whereas C–Pt sigma bonds on Pt surfaces are typically $\sim$ 75 kJ/mol stronger [17,18]. Because of the weakness of Bi–C bonds compared to Pt–C bonds, the barrier to many reactions with this species will decrease. Thus, coupling reactions between adsorbates become possible at much lower temperatures. At the same time, decomposition reactions requiring vacant Pt sites are curtailed. The end result is that adsorbate–adsorbate coupling becomes important, as opposed to group transfer to the substrate. Hence in the presence of Bi the barrier to benzyl coupling is reduced and C–C bond formation becomes feasible. Indeed, there are other examples of thermal or photolytic decomposition of organobismuth compounds leading to the dimers of the organic ligand [15], similar to what we see here. When adsorbed H is present, H–benzyl coupling occurs for the same reasons, plus the fact that H_a is also destabilized by the bismuth [5d].

In the absence of hydrogen, when benzyl dimerization appears to dominate as in normal BPTDS, some direct desorption of benzyl radicals also appears to occur. Competition between dimerization and evolution of gaseous radicals is not unprecedented [15,27]. Methyls adsorbed on Cu and Au surfaces desorb directly as radicals and also couple to give ethane at about the same temperature in TPD, with coadsorbate coverages controlling the ratio of yields [27].

The weakness of the Bi–C bond also explains why direct desorption of the benzyl radical is a competitive process even at this low temperature ($\sim$ 340 K for multilayer Bi). Fig. 4 is a plot which has allowed us to estimate the C–Bi bond strength in bismuth–benzyl complexes. It is based on the well-known correlation between metal–X (or M–X) bond strengths and H–X bond strengths [22], where "X" refers to an organic fragment like methyl or benzyl. As expected based on that correlation and shown in fig. 4, Sn–phenyl, Sn–methyl, Sn–ethyl and Sn–benzyl mean bond dissociation energies [#1] show a nearly linear plot with a slope of 1.0 versus the corresponding H–X bond dissociation energies, taken from ref. [23]. We estimated the Bi–benzyl mean bond dissociation energy to be $\sim$ 75 kJ/mol by extrapolating

[#1] Most of these values were taken from table 5 of ref. [13]. The Sn–phenyl mean bond dissociation energy was calculated using data from tables 1 and 2 in ref. [13] in the same way that the other values listed in table 5 of ref. [13] were calculated.

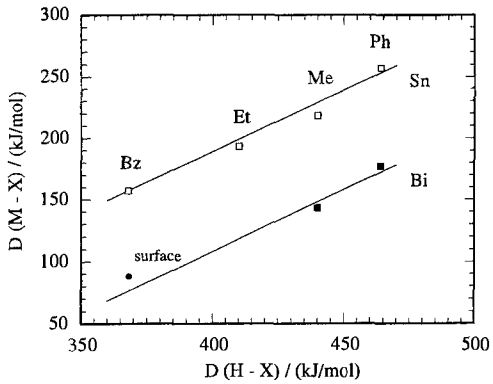

Fig. 4. Squares: Correlation of the mean M–C bond dissociation energy D(M–X), for various organic ligands in tin and bismuth complexes with H–C bond dissociation energy, D(H–C), for that same ligand attached to H in the gas phase. Values from ref. [13] and from ref. [23]. The lines show the slope of 1.00 expected based on such correlations with other metals [22]. Bz = benzyl, Et = ethyl, Me = methyl, Ph = phenyl. Round point: The Bi–C bond strength for surface benzyl, estimated by using the activation energy for benzyl radical desorption from multilayer Bi measured here.

the same type plot for bismuth from the known values for Bi–phenyl and Bi–methyl, again taken from ref. [13] and again assuming a slope of 1.0, as shown. Taking this value of 75 kJ/mol for the activation energy for desorption of benzyl radicals, Redhead analysis [12] gives a TPD peak temperature of only 297 K, assuming a typical first-order desorption preexponential factor of 10^{13} s^{-1}. This value of 75 kJ/mol is less than the activation energy estimated above for evolution of bibenzyl: 88 kJ/mol for multilayer Bi and 101 kJ/mol for 1 ML. Thus, it is not unreasonable that direct desorption of this radical should be a competitive process in BPTDS even at only 300–420 K. Since the extra intensities in the mass spectrum that are attributed to benzyl radical appear nearly simultaneously with bibenzyl in these peaks, these activation energies of 88 and 101 kJ/mol are also appropriate experimental estimates for benzyl radical desorption. By comparison to bismuth, Pt–C bond strengths are about 92 kJ/mol stronger [24], so radical desorption directly from Pt sites is much less likely.

In the estimation above, a question arises as to whether such carbon–metal bond strengths in organometallic complexes approximate the corresponding values in adsorbate bonding to metal surfaces. This was previously suggested to be the case [25], and thermodynamic estimates based on that assumption agree well with recent calorimetric measurements of heats of adsorption and reaction on Pt(111) [26]. Thus, we have entered a circular point in fig. 4 for the Bi–C bond strength for benzyl of 88 kJ/mol, estimated by using the activation energy for benzyl radical desorption from multilayer Bi, from above.

Novel chemistry has therefore been demonstrated through adsorption of Bi to a benzyl covered Pt surface. The reasons for this phenomenon are relatively easily understood. We have seen that if we can create an adsorbed radical species on the Pt surface, at a temperature below that at which further decomposition of this species by the Pt occurs, it is possible to induce a coupling reaction and, crucially, we can also induce desorption of the dimer product intact, and even of some of the monomer. The overall dimerization process is similar to the Ullman coupling reactions that occur over Cu catalysts [16]. However, those reactions require an electrophilic leaving group (for instance iodine) to generate the radical species on the surface. In the current case we can achieve radical formation and subsequent coupling from an aromatic hydrocarbon, or even from a suitable alkane, since Pt is the substrate. However, this process is certainly not catalytic as observed here. It would be interesting to see whether a suitable Bi coverage might be found where this process could actually be achieved catalytically. This would have to be a low enough coverage to allow some access of hydrocarbons to Pt sites so that C–H bond cleavage and benzyl formation could be accomplished, although perhaps slowly. At the same time, the coverage would have to be high enough to allow coupling and product desorption to occur. If this were possible, it would probably occur near one monolayer, and would certainly require greater than 1/2 ML (see above).

All three curves in fig. 2 give a measure of the amount of adsorbed benzyl as a function of the preflash temperature. As can be seen, the amount decreases to zero between 440 and 485 K, with a maximum slope near 475 K. Assuming a typical preexponential factor for adsorbate decomposition of 10^{11} s^{-1} [19], a simple first-order Redhead-type analysis of this peak temperature [12] yields an activation energy for benzyl decomposition of $\sim$ 104 kJ/mol. Note that this number is characteristic of *bismuth-free* Pt(111), since the preflash is done before Bi deposition. HREELS data indicate that the methylene side group on adsorbed benzyl is sp^3-hybridized [11]. It is surprising that this group survives to 475 K, since sp^3-hybridized C–H bonds in adsorbed hydrocarbons usually break at much lower temperatures during TPD on Pt(111) [4,5]. Indeed, this activation energy is much closer to the range expected for C–H cleavage at sp^2-type carbons (116–125 kJ/mol [4,21]) than at sp^3-type carbons ($\sim$ 60 kJ/mol [4,21]). The unusually high value here may be related to the large additional barrier expected to be experienced in rotating the C $\rightarrow$ H bond vector toward the surface, from its normal orientation away from the surface [11].

The following conclusions can be reached:

(1) Benzyl species, which can be produced on Pt(111) with methylcyclohexane or toluene, can be induced to couple and desorb as bibenzyl with high yield through the addition of Bi to the surface. This chemistry is absent on clean Pt, where its further decomposition is preferred.

(2) Bismuth facilitates this new chemistry through disruption of the benzyl–Pt bonding and, at the same time, suppression of the decomposition rate of adsorbed

benzyl. The barrier to the coupling reaction is significantly reduced. This correlates with the fact that benzyl–Pt bonds are apparently replaced with benzyl–bismuth bonds. The reduction in the activation energy for benzyl coupling is probably related to the well known weakness of carbon–bismuth bonds [13–15].

(3) The degree to which the barrier to C–C bond formation has been reduced is such that bibenzyl can be formed (from adsorbed benzyl) and desorbed from 1 ML Bi/Pt(111) by $\sim$ 400 K. We can set an upper limit of $\sim$ 101 kJ mol^{-1} on the activation energy for this process for 1 ML Bi/Pt(111).

(4) Higher Bi coverage makes the formation/desorption even more facile and product evolution is seen to occur at $\sim$ 340 K. This is due to the second layer of Bi further screening the adsorbates from the effect of the Pt, further destabilising the adsorbed benzyl relative to its energy on clean Pt. The upper limit to the barrier to the C–C bond formation reaction falls to $\sim$ 88 kJ mol^{-1} for 2 ML Bi/Pt(111).

(5) Some direct desorption of the benzyl radical also occurs, in competition with its dimerization.

(6) If coadsorbed hydrogen or deuterium adatoms are also present, their addition to benzyl to make toluene gas is more efficient than the coupling reaction and direct radical desorption, and it occurs at $\sim$ 210 K. However, the coupling reaction is reasonably efficient in the absence of H or D.

(7) The displacement of adsorbed hydrocarbons by an intervening bismuth layer helps us to understand how BPTDS operates as an analytical tool.

(8) In interpretting BPTDS spectra, the possibility for adsorbate coupling and radical desorption should be considered. These might even have utility in identifying adsorbates. However, these processes will generally require a higher activation energy and temperature than seen here with benzyl, due to the unusual weakness of the Bi–benzyl bond, which arises from the unusual stability of the benzyl radical [13]. (Estimates of the activation energies for other organic fragments could be made from fig. 4 for multilayer Bi, adding $\sim$ 13 kJ/mol based on the difference seen above: 88 vs. 75 kJ/mol. Another 13 kJ/mol should be added for monolayer Bi, based on the difference seen above: 101 vs. 88 kJ/mol.) Because they occur at higher temperatures, these processes are relatively easy to separate from normal BPTDS peaks for molecularly adsorbed organics, which occur below 300 K [5].

(9) The activation energy for benzyl decomposition on bismuth-free Pt(111) is $\sim$ 104 kJ/mol.

Acknowledgement

The authors acknowledge the National Science Foundation for financial support of this work. They gratefully thank Karen Goldberg, Mike Heinekey and Brian Bent for helpful discussions.

References

[1] M.C. McMaster and R.J. Madix, Surf. Sci. 275 (1992) 265;
F. Zaera, Surf. Sci. 262 (1992) 335; J. Phys. Chem 94 (1990) 5030, 8350;
M.A. Henderson, G.E. Mitchell and J.M. White, Surf. Sci. 248 (1991) 279.

[2] J. Clavilier, J.M. Feliu and A. Aldaz, J. Electroanal. Chem. 243 (1988) 419;
S.A. Campbell and R. Parsons, J. Chem. Soc. Faraday Trans. 88 (1992) 833.

[3] T. Mallat, Z. Bednar and A. Baiker, in: *Heterogeneous Catalysis and Fine Chemicals III*, eds. M. Guisnet et al. (Elsevier, Amsterdam, 1993).

[4] C.T. Campbell, J.M. Campbell, P.J. Dalton, F.C. Henn, J.A. Rodriguez and S.G. Seimanides, J. Phys. Chem. 93 (1989) 806, 815, 826, 836.

[5] (a)M.B. Hugenschmidt, M.E. Domagala and C.T. Campbell, J. Vac. Sci. Technol. A 10 (1992) 2556;
(b)F.C. Henn, A.L. Diaz, M.E. Bussell, M.B. Hugenschmidt, M.E. Domagala and C.T. Campbell, J. Phys. Chem. 96 (1992) 5965;
(c)M.E. Domagala and C.T. Campbell, Langmuir 10 (1994) 2636;
(d)M.E. Domagala and C.T. Campbell, Surf. Sci. 301 (1994) 151;
(e)C.T. Campbell, in: *Critical Reviews in Surface Chemistry* 4 (Begell House, 1994) 49;
(f)M.E. Domagala and C.T. Campbell, J. Vac. Sci. Technol. A11 (1993) 2128.

[6] L.Q. Jiang, A. Avoyan and B.E. Koel, J. Am. Chem. Soc. 225 (1993) 12106.

[7] C. Xu, B.E. Koel, N. Frei, M.A. Newton and C.T. Campbell, J. Phys. Chem., in press.

[8] M.A. Newton and C.T. Campbell, to be published.

[9] M.A. Newton and C.T. Campbell, unpublished data.

[10] F.W. McLafferty and D.B. Stauffer, *The Wiley/NBS Registry of Mass Spectral Data* (Wiley, New York, 1989); *Eight Peak Index of Mass Spectra*, 3rd Ed. (The Royal Society of Chemistry, Nottingham, 1983).

[11] N.R. Avery, J. Chem. Soc. Chem. Commun. (1988) 153.

[12] P.A. Redhead, Vacuum 12 (1962) 203.

[13] H.A. Skinner, Adv. Organomet. Chem. 2 (1964) 49.

[14] J.S. Thayer, *Organometallic Chemistry: An Overview* (VCH, Weinheim, 1987) p. 48.

[15] L.D. Freedman and G.O. Cook, Chem. Rev. 82 (1982) 15.

[16] M. Xi and B.E. Bent, J. Am. Chem. Soc. 115 (1993) 7426.

[17] E.A. Carter and B.E. Koel, Surf. Sci. 226 (1990) 339.

[18] A. Struck, E. Wartnaby, Y.Y. Yeo and D.A. King, Phys. Rev. Lett. 74 (1995) 578.

[19] C.T. Campbell, Y.-K. Sun and W.H. Weinberg, Chem. Phys. Lett. 179 (1991) 53.

[20] F. Turecek, Org. Mass Spec. 27 (1992) 1087.

[21] S.A. Shaffer and F. Turecek, to be published.

[22] H.E. Bryndza, L.K. Fong, R.A. Paciello, W. Tam and J.E. Bercaw, J. Am. Chem. Soc. 109 (1987) 1444.

[23] D.F. McMillen and D.M. Golden, Ann. Rev. Phys. Chem. 33 (1982) 493.

[24] J.A. Martinho Simoes and J.L. Beauchamp, Chem. Rev. 90 (1990) 629.

[25] E.A. Carter and B.E. Koel, Surf. Sci. 226 (1990) 339.

[26] A. Struck, C.E. Wartnaby, Y.Y. Yeo and D.A. King, Phys. Rev. Lett. 74 (1995) 578.

[27] A. Paul and B.E. Bent, J. Catal. 147 (1994) 267.